AD

AD-A211 834

TECHNICAL REPORT ARCCB-TR-89018

APPLICATIONS AND LIMITATIONS OF FINITE ELEMENT ANALYSIS TO ARMAMENT COMPONENTS

J. H. UNDERWOOD

JULY 1989

US ARMY ARMAMENT RESEARCH, DEVELOPMENT AND ENGINEERING CENTER
CLOSE COMBAT ARMAMENTS CENTER
BENÉT LABORATORIES
WATERVLIET, N.Y. 12189-4050

DISCLAIMER

The findings in this report are not to be construed as an official Department of the Army position unless so designated by other authorized documents.

The use of trade name(s) and/or manufacturer(s) does not constitute an official indorsement or approval.

DESTRUCTION NOTICE

For classified documents, follow the procedures in DoD 5200.22-M, Industrial Security Manual, Section II-19 or DoD 5200.1-R, Information Security Program Regulation, Chapter IX.

For unclassified, limited documents, destroy by any method that will prevent disclosure of contents or reconstruction of the document.

For unclassified, unlimited documents, destroy when the report is no longer needed. Do not return it to the originator.

SECURITY CLASSIFICATION OF THIS PAGE (When Data Entered)

REPORT DOCUMENTATION PAGE		READ INSTRUCTIONS BEFORE COMPLETING FORM
1. REPORT NUMBER ARCCB-TR-89018	2. GOVT ACCESSION NO.	3. RECIPIENT'S CATALOG NUMBER
4. TITLE (and Subtitle) APPLICATIONS AND LIMITATIONS OF FINITE ELEMENT ANALYSIS TO ARMAMENT COMPONENTS		5. TYPE OF REPORT & PERIOD COVERED Final 6. PERFORMING ORG. REPORT NUMBER
7. AUTHOR(s) J. H. Underwood		8. CONTRACT OR GRANT NUMBER(s)
9. PERFORMING ORGANIZATION NAME AND ADDRESS U.S. Army ARDEC Benet Laboratories, SMCAR-CCB-TL Watervliet, NY 12189-4050		10. PROGRAM ELEMENT, PROJECT, TASK AREA & WORK UNIT NUMBERS AMCMS No. 6126.24.1BL0.0AR PRON No. 1A72ZH7QNMSC
11. CONTROLLING OFFICE NAME AND ADDRESS U.S. Army ARDEC Close Combat Armaments Center Picatinny Arsenal, NJ 07806-5000		12. REPORT DATE July 1989 13. NUMBER OF PAGES 22
14. MONITORING AGENCY NAME & ADDRESS(if different from Controlling Office)		15. SECURITY CLASS. (of this report) UNCLASSIFIED 15a. DECLASSIFICATION/DOWNGRADING SCHEDULE

16. DISTRIBUTION STATEMENT (of this Report)

Approved for public release; distribution unlimited.

17. DISTRIBUTION STATEMENT (of the abstract entered in Block 20, if different from Report)

18. SUPPLEMENTARY NOTES

Presented at the Fifth International Conference in Australia on Finite Element Methods, University of Melbourne, 19-21 August 1987. Published in Proceedings of the Conference.

19. KEY WORDS (Continue on reverse side if necessary and identify by block number)

Finite Elements
Fracture Mechanics
Stress Analysis
Armament Components
Fracture Tests
Fatigue
Notch Stress

20. ABSTRACT (Continue on reverse side if necessary and identify by block number)

A review of three applications of finite element methods for stress, displacement, and stress intensity factor analyses of various armament components is presented. First, stress analysis of sections from outside diameter notched cylinders was performed to describe the cylinder's fatigue life behavior. Second, stress analysis methods for long rod projectiles subjected to inertial loading were developed; the stresses at a failure location of a projectile were used to help explain the failure and were related to results of mechanical

(CONT'D ON REVERSE)

DD FORM 1 JAN 73 1473 EDITION OF 1 NOV 65 IS OBSOLETE

UNCLASSIFIED

SECURITY CLASSIFICATION OF THIS PAGE (When Data Entered)

20. ABSTRACT (CONT'D)

tests of the projectile and the projectile material. Last, stress intensity factor and displacement analyses of fracture mechanics test specimens were performed to recommend standardized test procedures. Stress intensity factor and load-line displacement solutions were obtained for three-point bend, arc-shaped specimens which can be conveniently cut from cylindrical vessels and pipes. The finite element solutions were compared with collocation solutions for the same and similar geometries.

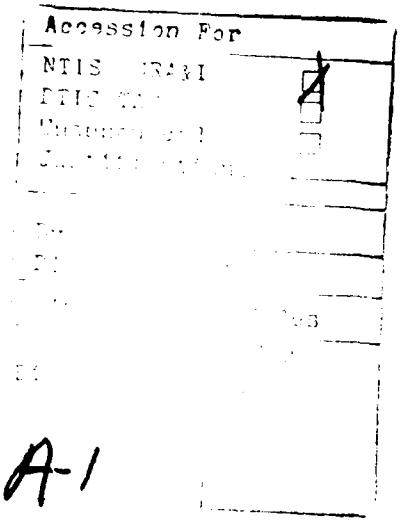

TABLE OF CONTENTS

TABLES

LIST OF ILLUSTRATIONS

INTRODUCTION

Finite element methods are used extensively for structural analysis of the basic components of armament, cannon tubes, and projectiles. When the loading or geometry of the component is so complex that available solutions do not directly apply, finite element analysis is an obvious choice. The primary objective here is to describe three recent applications of finite elements to armament, with emphasis on both the finite element methods and the engineering application. A secondary objective is to discuss some special requirements and limitations associated with the use of finite elements for structural analysis of weapon components.

The first of the three applications, a notched component (ref 1), is a common application of finite elements. The fundamental geometry considered, a pressurized cylinder, is often the subject of pressure vessel and piping investigations. The main point of this first example is the relationship of the stress analyses results to those from fracture mechanics testing and analyses which address the cylinder's fatigue life. The second application, a two-body component subjected to inertial loading (ref 2), is a complex structural problem with little similar prior work for guidance. A long rod projectile was analyzed using certain assumptions to describe the interconnection between the two basic parts of the projectile. Again, the results were related to the mechanical and fracture test results from the actual component. The third topic has a more

[1] J. A. Kapp and J. H. Underwood, "Service Simulation Tests to Determine the Fatigue Life of OD Notched Thick-Wall Cylinders," Experimental Mechanics, Vol. 22, No. 3, March 1982, pp. 96-100 (also ARLCB-TR-82008, U.S. Army ARRADCOM, Benet Weapons Laboratory, Watervliet, NY, April 1982).

[2] J. H. Underwood and M. A. Scavullo, "Fracture Behavior of a Uranium and a Tungsten Alloy in a Notched Component With Inertia Loading," Fracture Mechanics: Sixteenth Symposium, ASTM STP 868, American Society for Testing and Materials, Philadelphia, PA, 1985, pp. 554-568 (also ARLCB-TR-83043, U.S. Army ARDC, Benet Weapons Laboratory, Watervliet, NY, December 1983).

general application. Finite element methods were used to obtain the stress intensity factor and two types of displacement results for a variety of fracture mechanics test geometries (ref 3). The results were compared with prior data, primarily boundary value collocation results, in order to verify and recommend some standardized test procedures.

CANNON TUBE EXAMPLE

Analysis and Test Conditions

Notches are sometimes cut into the outside diameter (OD) surface of a cannon tube. Since the circumferential stress on the OD surface due to firing and overstrain (ref 1) are both tensile, an OD notch is often the initiation point of cracking. Fatigue cracks initiate at the notch root and, if ignored, can lead to a final, fast growth of the crack through the tube wall. To help describe and predict the fatigue crack initiation, finite element analysis was performed on the notched tube geometry, as shown in Figure 1. Quadrilateral two-dimensional plate and constant strain triangle elements were used. The analysis was conducted using the NASTRAN program on an IBM 360/44 machine. To accurately determine the stresses at the root of the notch, it was necessary to refine the grid (Figure 2). The overall geometry modeled was a test specimen which simulated the key features of a pressurized cylinder and was more easily tested than a full-size pressurized cylinder. Several simulation specimens of this type were made and tested from one cylinder to determine fatigue lives

[1] J. A. Kapp and J. H. Underwood, "Service Simulation Tests to Determine the Fatigue Life of OD Notched Thick-Wall Cylinders," Experimental Mechanics, Vol. 22, No. 3, March 1982, pp. 96-100 (also ARLCB-TR-82008, U.S. Army ARRADCOM, Benet Weapons Laboratory, Watervliet, NY, April 1982).

[3] J. H. Underwood, J. A. Kapp, and M. D. Witherell, "Fracture Testing With Arc Bend Specimens," Fracture Mechanics: Seventeenth Volume, ASTM STP 905, American Society for Testing and Materials, Philadelphia, PA, 1986, pp. 279-296 (also ARLCB-TR-85014, U.S. Army ARDC, Benet Weapons Laboratory, Watervliet, NY, May 1985).

under various conditions. The fatigue load, P, was chosen to produce the same approximate value of the notch root stress in the simulation specimen as that caused by the firing and overstrain loading of the tube.

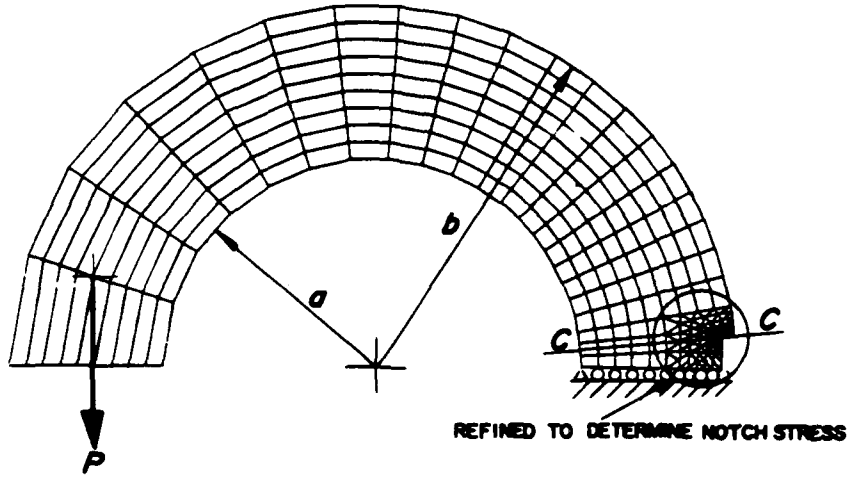

Figure 1. Finite element grid of test specimen for simulation of notched cylinder.

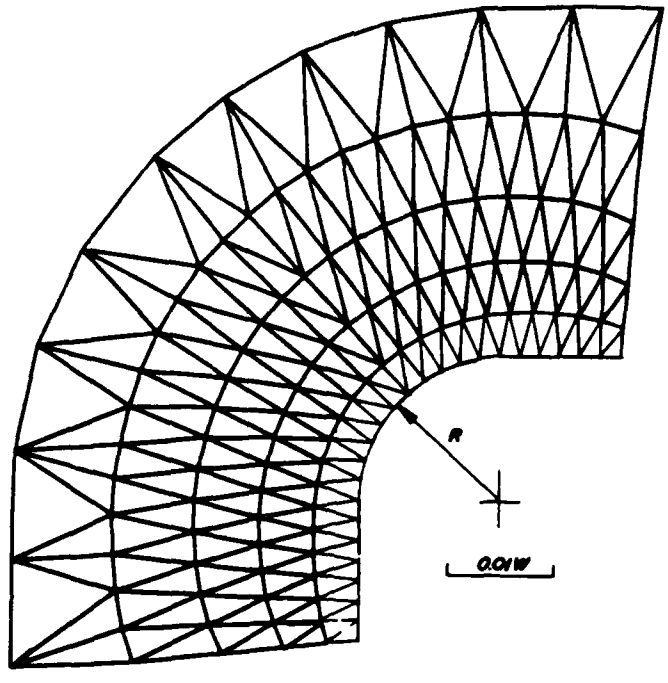

Figure 2. Refined grid around the notch root.

Finite Element Resul

Figure 3 summarizes the test specimen geometry and a representative set of finite element results for a notch depth, c = 10 mm. The radial distribution of the circumferential direction stress, σ, in a nondimensional form along the line C-C is plotted from a point near the inner diameter (ID) surface to just below the notch root surface. Since the notch depth for these results was 10 mm, the notch root is at the position r = 125 mm. The significant concentration of stress at the notch location can be seen as r approaches 125 mm.

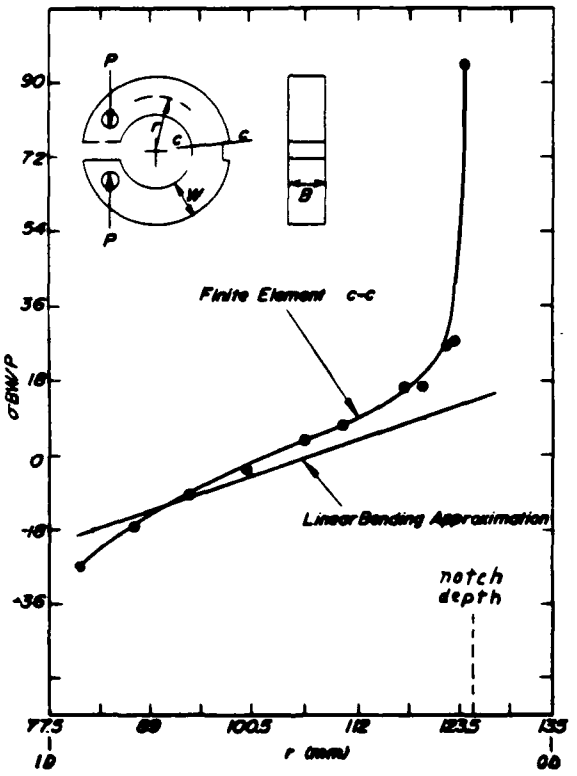

Figure 3. Summary of test specimen geometry and radial distribution of circumferential direction stress from finite element and linear bending analyses.

It is interesting to compare the finite element results, including the substantial effects of the notch, to a linear bending analysis of the specimen which assumes that no notch is present

$$\sigma_{nom} = -\frac{P}{BW} + \left[\frac{6PX}{BW^2}\right]\left[\frac{2(r-a)}{W} - 1\right] \quad (1)$$

In the linear bending analysis described by Eq. (1), σ_{nom} is the circumferential stress and X is the moment arm between the load line and mid-wall thickness position at the notch location. The other parameters define the specimen geometry with values: a = 77.5 mm, B = 50 mm, W = 57.5 mm, X = 196 mm. The comparison of the linear bending results with finite elements results in Figure 3 shows relatively small differences away from the notch and larger differences due to stress concentration near the notch.

Relation to Fatigue Life

Fatigue life tests were performed using a specimen as shown in Figure 3 with notch depths of 10 and 5 mm, a constant notch width of 25.4 mm, and a root radius, R, of 1.5 mm. Fatigue life here was the total number of cycles to initiate and grow the crack to complete failure. The results in Table I show more than a threefold increase in fatigue life corresponding to a halving of the notch depth. Since the maximum stress at the notch root is a controlling factor for fatigue crack initiation, finite element calculation of the notch root stress should help in describing fatigue behavior. Calculations for two notch depths are shown in Table I. Also shown is a fracture mechanics calculation of notch root stress using the method of Rolfe and Barsom (ref 4). They used the following approximation for notch root stress:

$$\sigma = 2K/(\pi R)^{\frac{1}{2}} \quad (2)$$

where K is the stress intensity factor. Combining Eqs. (1) and (2) with the

[4]S. T. Rolfe and J. H. Barsom, Fracture and Fatigue Control in Structures, Prentice Hall, Englewood Cliffs, NJ, 1977.

well-known expression for K for a shallow edge crack (ref 5) of depth c,

$$K = 1.12\ \sigma_{nom}(\pi c)^{1/2}$$

gives the values listed in Table I. Note that the finite element results are about 12 percent below the $K/R^{1/2}$ results. This may be due to the fact that the finite element results are for a position slightly below the notch root surface.

TABLE I. MEASURED FATIGUE LIFE AND CALCULATED NOTCH-TIP STRESS FOR CYLINDER SECTIONS

Notch Depth c mm	Fatigue Life		Maximum Stress at Notch	
	Two Tests N Cycles	Mean N Cycles	Finite Element Analysis σBW/P	$K/R^{1/2}$ Analysis σBW/P
10	2,752 3,288	3,020	95	107
5	9,280 11,224	10,252	66	76

A useful description of fatigue life, N, can often be obtained from (ref 1)

$$N = \text{constant}\ (\sigma)^{-3} \qquad (3)$$

Using Eq. (3) and the σ values from Table I, the predicted increases in fatigue life due to halving the notch depth were factors of 2.98 and 2.79 for the finite element and $K/R^{1/2}$ analyses, respectively. The measured increase in fatigue life was a factor of 3.39. Based on this relatively good agreement between prediction and measurement, both the finite element and $K/R^{1/2}$ analyses can be used to describe geometry effects on the fatigue life of a notched cylinder.

[1] J. A. Kapp and J. H. Underwood, "Service Simulation Tests to Determine the Fatigue Life of OD Notched Thick-Wall Cylinders," Experimental Mechanics, Vol. 22, No. 3, March 1982, pp. 96-100 (also ARLCB-TR-82008, U.S. Army ARRADCOM, Benet Weapons Laboratory, Watervliet, NY, April 1982).

[5] H. Tada, P. C. Paris, and G. R. Irwin, The Stress Analysis of Cracks Handbook, Del Research Corporation, Hellertown, PA, 1973.

PROJECTILE EXAMPLE

Finite Element Model and Results

The general modeling of a cannon projectile under service loading conditions can only be conducted adequately by using a two-dimensional method such as finite element analysis. The combination of geometry and loading is nearly always too complex for anything less. The projectile example described here is a typical long rod projectile made up of two basic components, the cylindrically-shaped rod and the segmented sabot which interconnects with the rod. The cannon firing pressure impinges to a greater extent on the sabot which transfers the resulting force to the rod. The purpose of the stress analysis was to calculate the acceleration stresses in the rod to understand and describe the rod failures which occasionally occur. Figure 4 shows the finite element

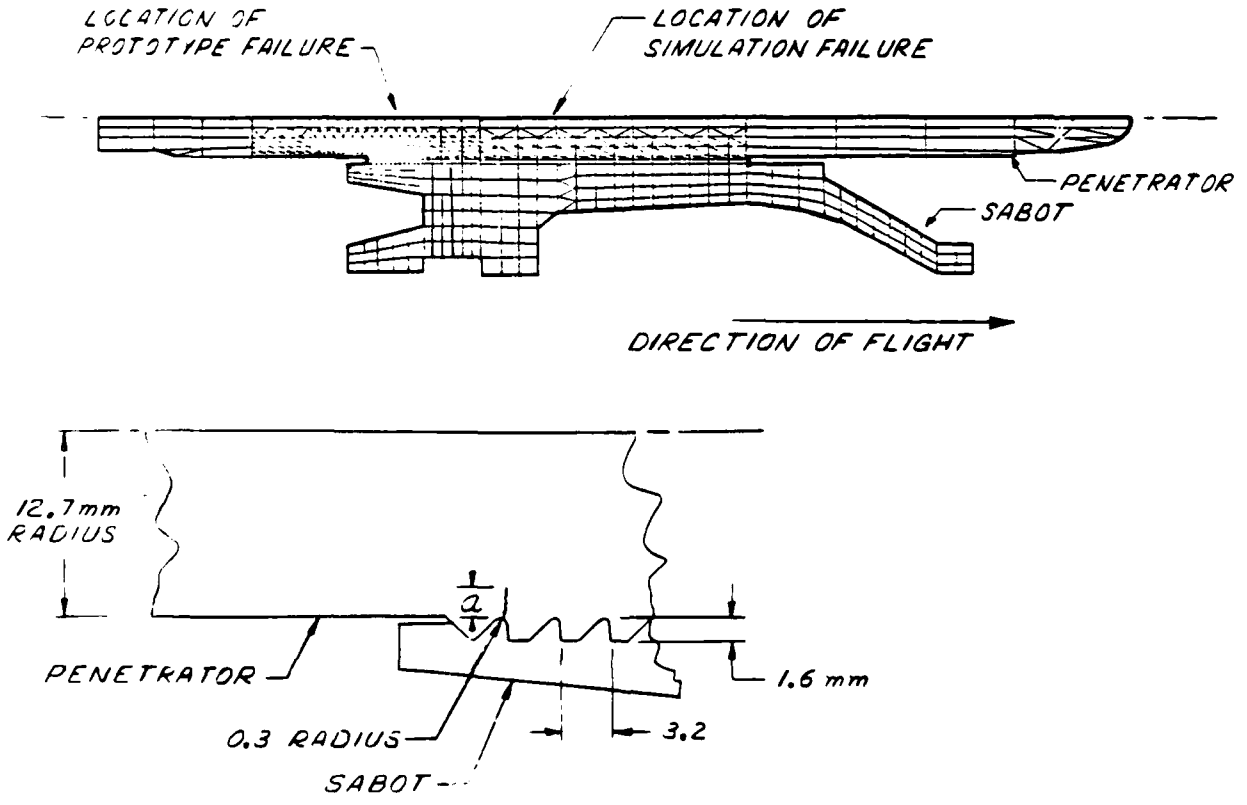

Figure 4. Finite element grid and sketch of portions of a long rod penetrator projectile.

grid used and some additional information about the projectile, its operation, and failure. As in the first example, both constant strain triangular and high order quadrilateral elements were used. The specific problem modeled was the tensile failure of a prototype uranium alloy rod at the root of the first of several lugs and grooves which transfer the forces between sabot and rod. The forces on the projectile at failure in this case were primarily due to acceleration. However, the pressure-induced loads in the radial direction can have a significant effect on the force transfer between the sabot and the rod. Plastic deformation and shifting of the regions of contact can occur, requiring assumptions about the amount of force transfer at any given point.

Figure 5 shows the axial distribution of axial direction stress, σ_z, up to the point of first contact between the sabot and rod. Up to this point, σ_z is little affected by the uncertainties of force transfer. The σ_z from the finite element model near the surface of the rod is compared with the following simple relation from mechanics:

$$\sigma_z = p + \frac{wG}{A} \tag{4}$$

where p is the cannon pressure, w is the weight of a given length of rod, G is a relative acceleration made dimensionless when normalized by the gravitational acceleration, and A is the area of the rod. The plot of Eq. (4) shown in Figure 5 corresponds to a relative acceleration of 34,000, not untypical of cannon firing. The generally higher values of σ_z from the finite element model are believed to arise from the inclusion of the weight of a tail fin assembly in that model, whereas no such effect is included in Eq. (4). The maximum axial stress from the finite element model was near the point of first contact with the sabot (the first lug), which was also the location of the failure. This stress was used to calculate the stress intensity factor and to determine a

minimum required fracture toughness for the uranium alloy. The measured fracture toughness from the lot of rods which included the failure was 18 MPa $m^{\frac{1}{2}}$. Following the incorporation of a minimum fracture toughness of 33 MPa $m^{\frac{1}{2}}$ as a material acceptance requirement, no further rod failures have occurred.

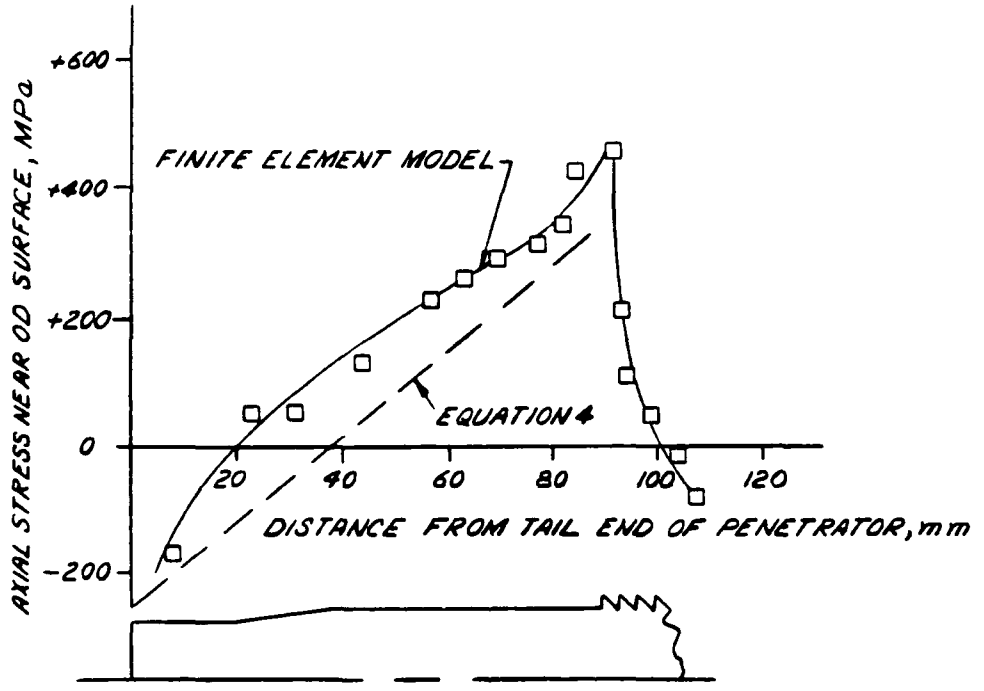

Figure 5. Axial distribution of axial direction stress near the surface of a penetrator subjected to launch acceleration.

Full-Scale Component Testing

A series of tests and analyses was conducted with full-scale penetrator rods to complement the finite element analysis. A tensile failure test of a penetrator rod was developed, as shown in Figure 6, and performed on both uranium and tungsten alloy rods. Plots of load versus deflection were recorded up to the failure point, and the total energy required to fail the penetrator was found to be a good indicator of failure during cannon firing. For example, in

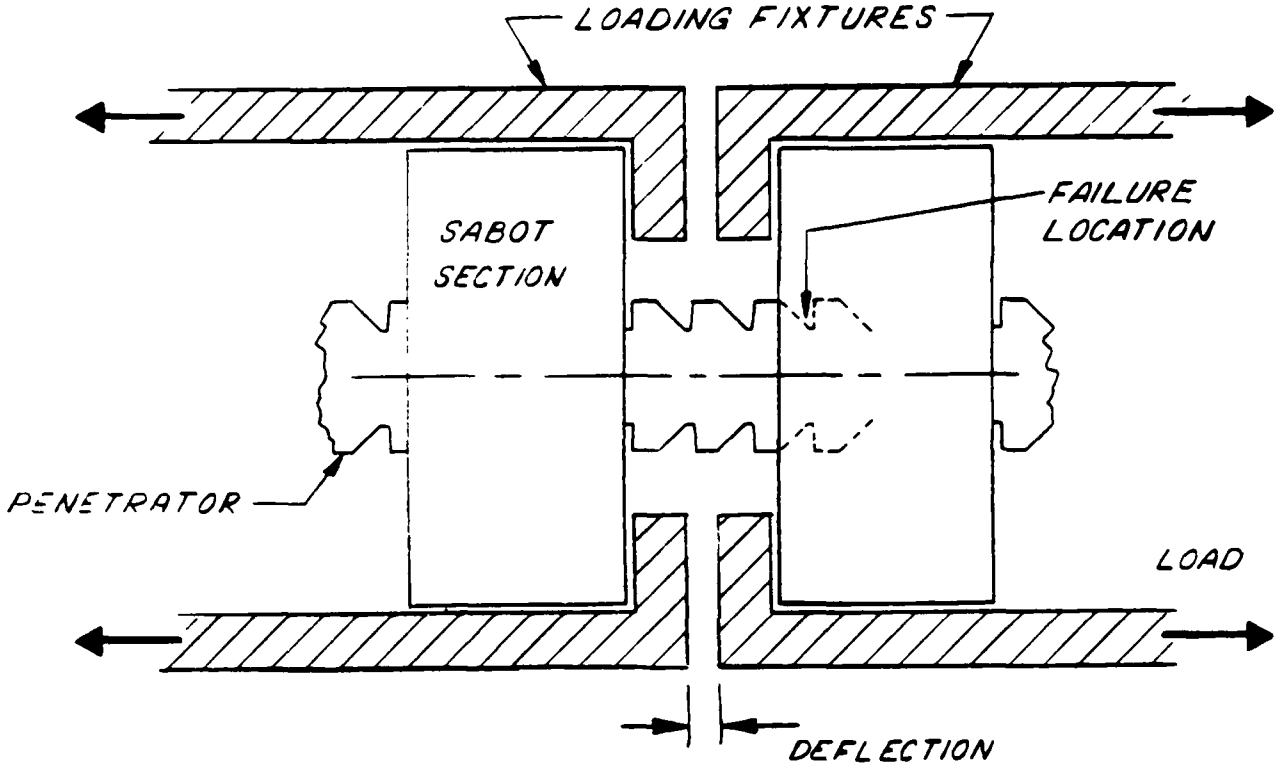

Figure 6. Sketch of arrangement for full-scale tensile failure tests of a penetrator.

Figure 7 the tungsten penetrator which failed at 410 KN, with a total area under the plot of less than 300 Nm, was one of a group which often failed during firing. The fracture toughness was measured from two groups of tungsten penetrators, the one which often failed during firing and one which did not fail. The results in Figure 8 show a high positive correlation between fracture toughness and failure energy of the full-scale penetrator. Table II summarizes this data along with other results. In general, the tests from a smooth tensile bar correlated poorly with the failure energy of the full-size rod, which contained the notch-like lugs and grooves. Fracture toughness tests, based on a notch and crack, correlated well.

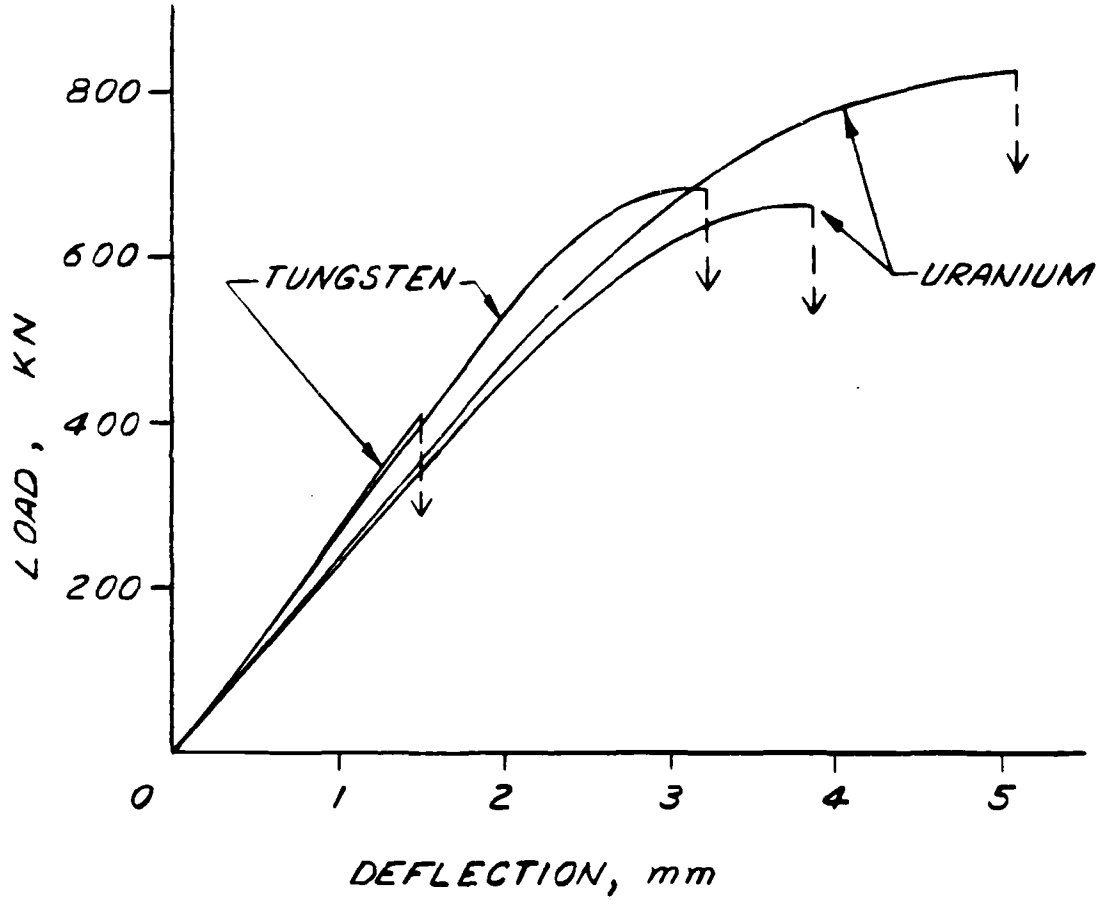

Figure 7. Load versus deflection plots of tungsten and uranium penetrators loaded to tensile failure.

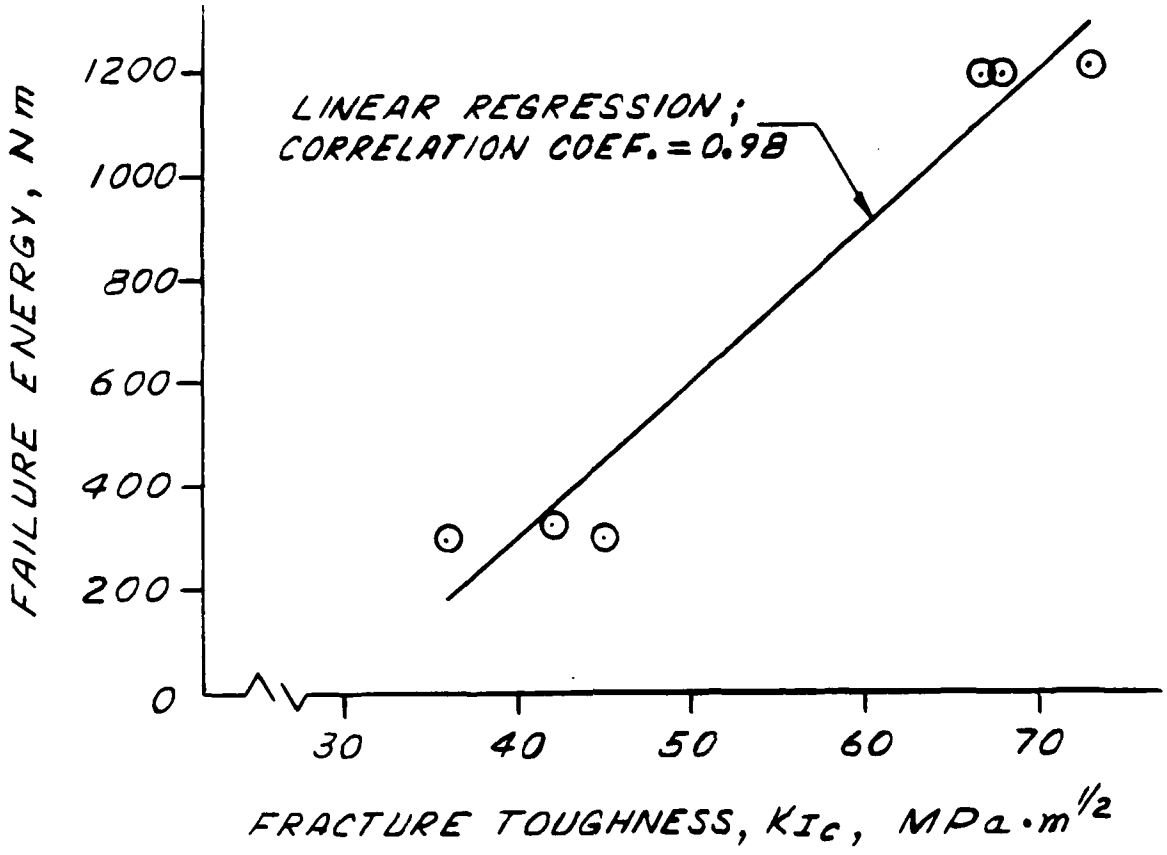

Figure 8. Relation between tensile failure energy of tungsten penetrators and fracture toughness of the penetrator material.

TABLE II. CORRELATION COEFFICIENT, r FROM n REPEAT TESTS: CORRELATION OF THREE MECHANICAL TESTS WITH THE TENSILE FAILURE ENERGY OF FULL-SIZE TUNGSTEN PENETRATOR RODS

Tensile Elongation		Reduction-in-Area		Fracture Toughness	
n	r	n	r	n	r
12	+0.68	12	+0.77	6	+0.98

It is interesting to note the general agreement between the stress analysis approach, that is, using finite elements to calculate the applied stress and the stress intensity factor, and the complementary approach of full-scale testing. Stress analysis was used to set a minimum fracture toughness which has successfully eliminated launch failures. Full-scale tests which simulate launch loading correlate well with the same material property fracture toughness. This agreement provides strong verification that finite element analysis can be used to directly describe full-component behavior of complex projectiles subjected to launch acceleration. The agreement also shows the value of full-scale testing to help answer difficult modeling questions. In the full-scale tests, the load was applied to the penetrator by way of the lugs, and thus the tests modeled some of the key aspects of the interconnection between the sabot and the penetrator rod.

FRACTURE MECHANICS TEST METHODS

Specimen Geometries and Finite Element Methods

Sections of cylinders are convenient fracture test specimens for armament components. One type of cylinder section extensively used has been standardized (ref 6). It is the arc tension specimen, a hollow cylinder section with a notch from the ID surface, loaded in tension by way of added holes. The topic of this third example of finite element applications is the development of three-point bend specimens from sections of cylinders. Some recent work (ref 3) used finite

[3] J. H. Underwood, J. A. Kapp, and M. D. Witherell, "Fracture Testing With Arc Bend Specimens," Fracture Mechanics: Seventeenth Volume, ASTM STP 905, American Society for Testing and Materials, Philadelphia, PA, 1986, pp. 279-296 (also ARLCB-TR-85014, U.S. Army ARDC, Benet Weapons Laboratory, Watervliet, NY, May 1985).

[6] "Standard Test Method for Plane-Strain Fracture Toughness of Metallic Materials, ASTM E-399," 1986 Annual Book of ASTM Standards, Vol. 03.01, American Society for Testing and Materials, Philadelphia, PA, 1986, pp. 522-557.

element methods to obtain stress and displacement results for a variety of proposed bend specimen geometries.

Figure 9 shows the two types of specimen geometries which were considered, both referred to as arc bend specimens, one supported on the ID arc surface and the other supported on a chordal surface. Accurate calculations of the stress intensity factor, K, crack mouth opening displacement, v, and load-line displacement, δ, are required for the various types of fracture tests which can be performed with a given specimen. The finite element grid which was used initially to calculate K, shown in Figure 10, is made up of 11 high order quadrilateral elements and 2 singular elements around the crack tip. It was considered necessary to add more elements, for a total of 29, for the v and δ calculations.

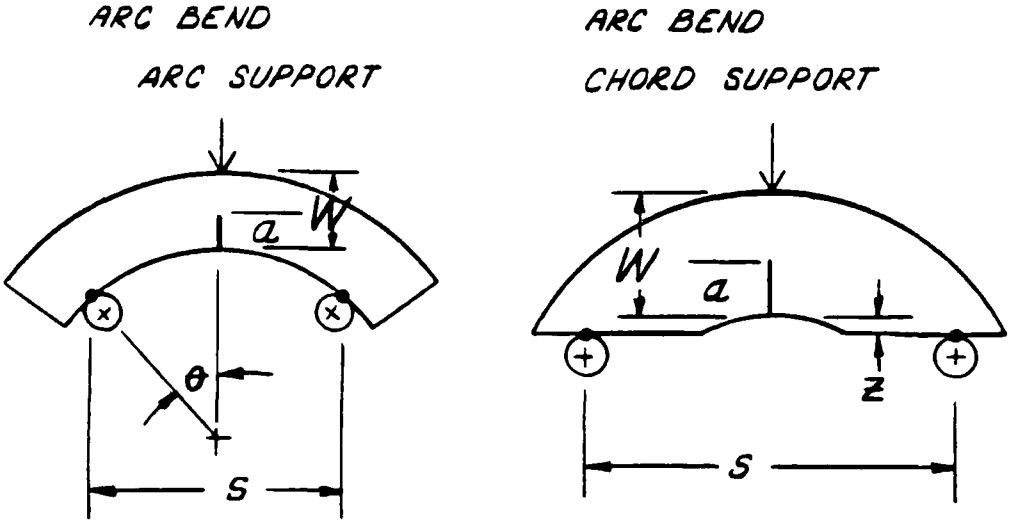

Figure 9. Sketch of arc bend-arc support and arc bend-chord support specimens for fracture testing.

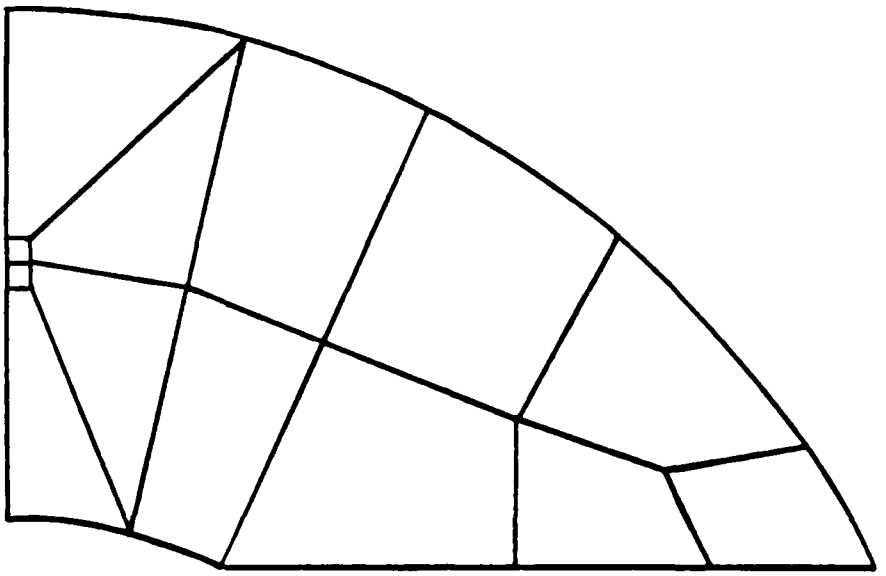

Figure 10. Finite element grid used for stress intensity factor and displacement calculations for arc bend-chord support specimen.

Limit Solutions for Bend Specimens

It is often a significant advantage to tailor the form of K, v, and δ results from a cracked specimen to the set of limit solutions for a deep crack in a semi-infinite body. Two of these solutions are (ref 5)

$$KBW^{1/2}/P = \frac{0.994\,(S/W)}{(1-a/W)^{3/2}} \tag{5}$$

$$EB\delta/P = \frac{0.988(S/W)^2}{(1-a/W)^2} \tag{6}$$

[5] H. Tada, P. C. Paris, and G. R. Irwin, The Stress Analysis of Cracks Handbook, Del Research Corporation, Hellertown, PA, 1973.

Equations (5) and (6) are exact only for deep cracks, that is, a/W approaching unity. However, they have the useful property of a nearly constant value over a wide range of a/W, particularly in the range 0.5 to 1.0. Note that the parameters Y and Y_δ in Figures 11 and 12 are generally close to the constants in Eqs. (5) and (6). This is because for $\theta = 0$, the form of Y and Y_δ was based on these limit solution equations. The use of these K and δ parameters with their nearly constant value allows simple and direct comparisons of various geometries, and also helps in obtaining accurate wide range expressions for K and δ results.

Finite Element Results

The K and δ data in Figures 11 and 12 provide several direct comparisons of finite element results with collocation results, as well as checks of both results with the deep crack limit solutions. Note the change in notation from that used earlier. In Figures 11 and 12, the inner and outer radii are r_1 and r_2, respectively.

In general, all comparisons of the K results in Figure 11 are very good. The collocation and finite element data of Figures 11(a) and (b) agree within 2 percent and all the data converge toward the exact deep crack limit. The comparisons of the δ data in Figure 12 are reasonable, but not as good as those for the K data. However, more variation in δ results is expected because the total δ is the sum of several components, both crack-related and whole specimen-related, whereas K is strongly controlled by the presence of the crack. The comparison of the finite element and collocation results in Figure 12(a) reveals some of this variation, resulting in a 7 percent difference between the two results for a/W = 0.7. For this relatively deep crack, the convergence of the results to the deep crack limit is a particularly useful check, because the limit solution is becoming more accurate and both the finite element and collocation results are becoming less accurate.

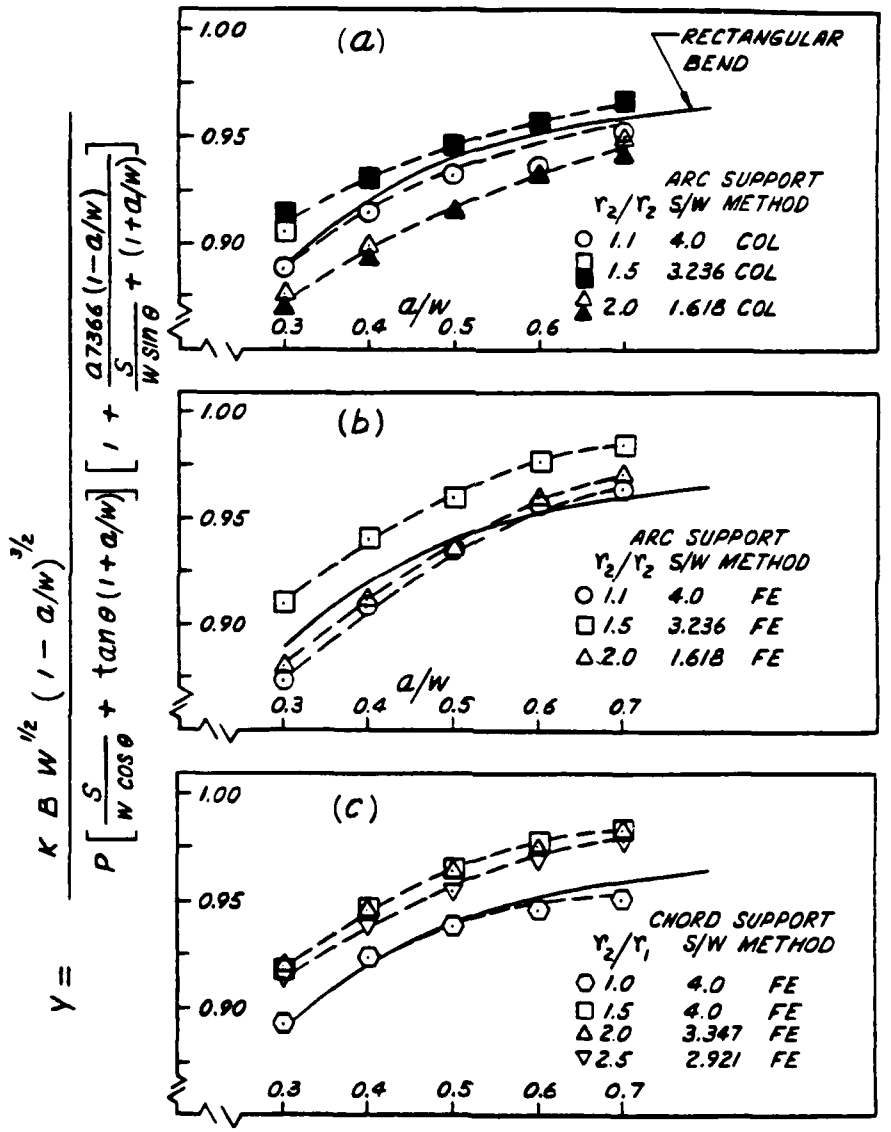

Figure 11. Plots of a stress intensity factor parameter from collocation and finite element analyses.

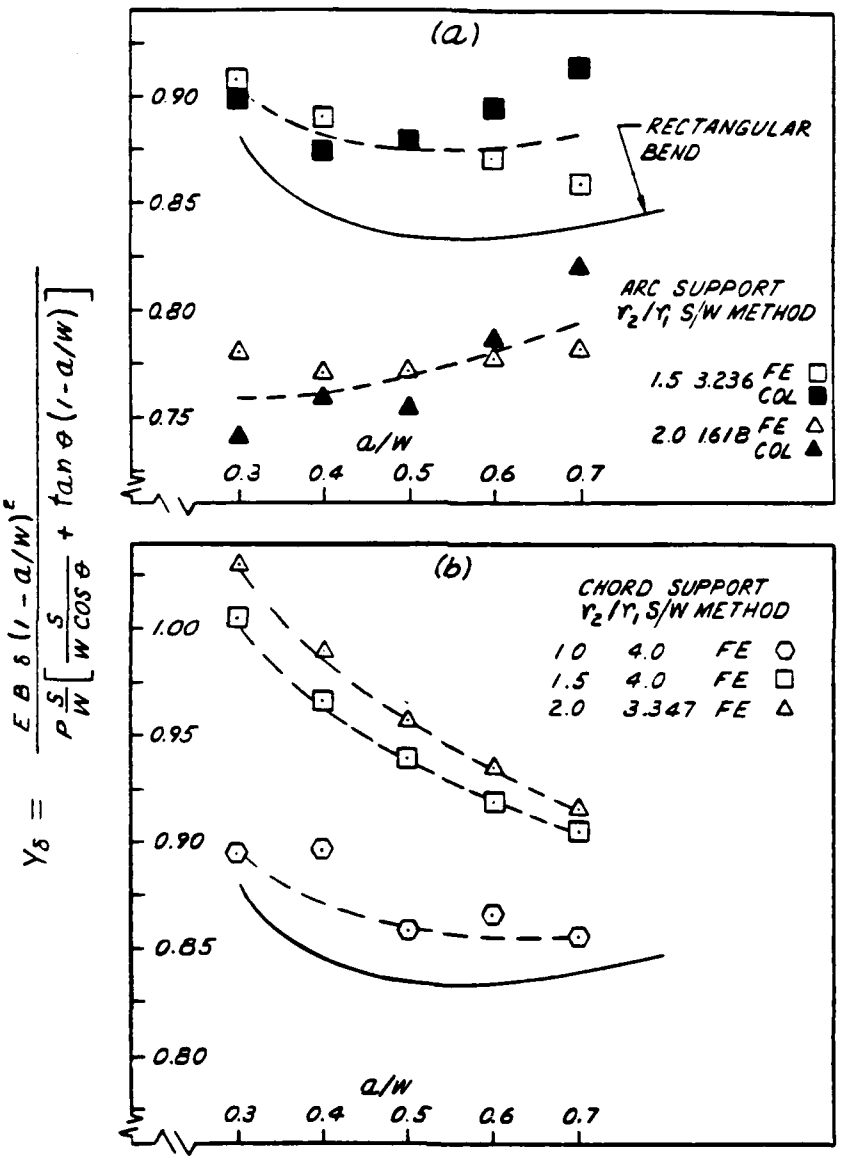

Figure 12. Plots of a load-line displacement parameter from collocation and finite element analyses.

CONCLUSIONS

The one general conclusion that can be reached from the review and evaluation of these three different applications is that checks of finite element results with known limit solutions continue to have great merit.

For the notched cylinder, a linear bending model of the cylinder wall was a useful comparison away from the notch, and a fracture mechanics approximation of the notch root stress compared favorably with the finite element results.

For the long rod, simple mechanics and the value of the applied acceleration relative to gravity gave an expression which agreed well with a complex finite element model.

For the cylinder section bend specimens, the detailed comparison of a variety of K and δ results would not have been possible without the use of deep crack limit solutions.

REFERENCES

1. J. A. Kapp and J. H. Underwood, "Service Simulation Tests to Determine the Fatigue Life of OD Notched Thick-Wall Cylinders," Experimental Mechanics, Vol. 22, No. 3, March 1982, pp. 96-100 (also ARLCB-TR-82008, U.S. Army ARRADCOM, Benet Weapons Laboratory, Watervliet, NY, April 1982).

2. J. H. Underwood and M. A. Scavullo, "Fracture Behavior of a Uranium and a Tungsten Alloy in a Notched Component With Inertia Loading," Fracture Mechanics: Sixteenth Symposium, ASTM STP 868, American Society for Testing and Materials, Philadelphia, PA, 1985, pp. 554-568 (also ARLCB-TR-83043, U.S. Army ARDC, Benet Weapons Laboratory, Watervliet, NY, December 1983).

3. J. H. Underwood, J. A. Kapp, and M. D. Witherell, "Fracture Testing With Arc Bend Specimens," Fracture Mechanics: Seventeenth Volume, ASTM STP 905, American Society for Testing and Materials, Philadelphia, PA, 1986, pp. 279-296 (also ARLCB-TR-85014, U.S. Army ARDC, Benet Weapons Laboratory, Watervliet, NY, May 1985).

4. S. T. Rolfe and J. H. Barsom, Fracture and Fatigue Control in Structures, Prentice Hall, Englewood Cliffs, NJ, 1977.

5. H. Tada, P. C. Paris, and G. R. Irwin, The Stress Analysis of Cracks Handbook, Del Research Corporation, Hellertown, PA, 1973.

6. "Standard Test Method for Plane-Strain Fracture Toughness of Metallic Materials, ASTM E-399," 1986 Annual Book of ASTM Standards, Vol. 03.01, American Society for Testing and Materials, Philadelphia, PA, 1986, pp. 522-557.

TECHNICAL REPORT INTERNAL DISTRIBUTION LIST

	NO. OF COPIES
CHIEF, DEVELOPMENT ENGINEERING DIVISION	
ATTN: SMCAR-CCB-D	1
-DA	1
-DC	1
-DM	1
-DP	1
-DR	1
-DS (SYSTEMS)	1
CHIEF, ENGINEERING SUPPORT DIVISION	
ATTN: SMCAR-CCB-S	1
-SE	1
CHIEF, RESEARCH DIVISION	
ATTN: SMCAR-CCB-R	2
-RA	1
-RM	1
-RP	1
-RT	1
TECHNICAL LIBRARY ATTN: SMCAR-CCB-TL	5
TECHNICAL PUBLICATIONS & EDITING SECTION ATTN: SMCAR-CCB-TL	3
DIRECTOR, OPERATIONS DIRECTORATE ATTN: SMCWV-OD	1
DIRECTOR, PROCUREMENT DIRECTORATE ATTN: SMCWV-PP	1
DIRECTOR, PRODUCT ASSURANCE DIRECTORATE ATTN: SMCWV-QA	1

NOTE: PLEASE NOTIFY DIRECTOR, BENET LABORATORIES, ATTN: SMCAR-CCB-TL, OF ANY ADDRESS CHANGES.

TECHNICAL REPORT EXTERNAL DISTRIBUTION LIST

	NO. OF COPIES
ASST SEC OF THE ARMY RESEARCH AND DEVELOPMENT ATTN: DEPT FOR SCI AND TECH THE PENTAGON WASHINGTON, D.C. 20310-0103	1
ADMINISTRATOR DEFENSE TECHNICAL INFO CENTER ATTN: DTIC-FDAC CAMERON STATION ALEXANDRIA, VA 22304-6145	12
COMMANDER US ARMY ARDEC ATTN: SMCAR-AEE	1
SMCAR-AES, BLDG. 321	1
SMCAR-AET-O, BLDG. 351N	1
SMCAR-CC	1
SMCAR-CCP-A	1
SMCAR-FSA	1
SMCAR-FSM-E	1
SMCAR-FSS-D, BLDG. 94	1
SMCAR-IMI-I (STINFO) BLDG. 59 PICATINNY ARSENAL, NJ 07806-5000	2
DIRECTOR US ARMY BALLISTIC RESEARCH LABORATORY ATTN: SLCBR-DD-T, BLDG. 305 ABERDEEN PROVING GROUND, MD 21005-5066	1
DIRECTOR US ARMY MATERIEL SYSTEMS ANALYSIS ACTV ATTN: AMXSY-MP ABERDEEN PROVING GROUND, MD 21005-5071	1
COMMANDER HQ, AMCCOM ATTN: AMSMC-IMP-L ROCK ISLAND, IL 61299-6000	1
COMMANDER ROCK ISLAND ARSENAL ATTN: SMCRI-ENM ROCK ISLAND, IL 61299-5000	1
DIRECTOR US ARMY INDUSTRIAL BASE ENGR ACTV ATTN: AMXIB-P ROCK ISLAND, IL 61299-7260	1
COMMANDER US ARMY TANK-AUTMV R&D COMMAND ATTN: AMSTA-DDL (TECH LIB) WARREN, MI 48397-5000	1
COMMANDER US MILITARY ACADEMY ATTN: DEPARTMENT OF MECHANICS WEST POINT, NY 10996-1792	1
US ARMY MISSILE COMMAND REDSTONE SCIENTIFIC INFO CTR ATTN: DOCUMENTS SECT, BLDG. 4484 REDSTONE ARSENAL, AL 35898-5241	2
COMMANDER US ARMY FGN SCIENCE AND TECH CTR ATTN: DRXST-SD 220 7TH STREET, N.E. CHARLOTTESVILLE, VA 22901	1
COMMANDER US ARMY LABCOM MATERIALS TECHNOLOGY LAB ATTN: SLCMT-IML (TECH LIB) WATERTOWN, MA 02172-0001	2

NOTE: PLEASE NOTIFY COMMANDER, ARMAMENT RESEARCH, DEVELOPMENT, AND ENGINEERING CENTER, US ARMY AMCCOM, ATTN: BENET LABORATORIES, SMCAR-CCB-TL, WATERVLIET, NY 12189-4050, OF ANY ADDRESS CHANGES.

TECHNICAL REPORT EXTERNAL DISTRIBUTION LIST (CONT'D)

	NO. OF COPIES
COMMANDER US ARMY LABCOM, ISA ATTN: SLCIS-IM-TL 2800 POWDER MILL ROAD ADELPHI, MD 20783-1145	1
COMMANDER US ARMY RESEARCH OFFICE ATTN: CHIEF, IPO P.O. BOX 12211 RESEARCH TRIANGLE PARK, NC 27709-2211	1
DIRECTOR US NAVAL RESEARCH LAB ATTN: MATERIALS SCI & TECH DIVISION CODE 26-27 (DOC LIB) WASHINGTON, D.C. 20375	1 1
COMMANDER AIR FORCE ARMAMENT LABORATORY ATTN: AFATL/MN EGLIN AFB, FL 32542-5434	1
COMMANDER AIR FORCE ARMAMENT LABORATORY ATTN: AFATL/MNF EGLIN AFB, FL 32542-5434	1
METALS AND CERAMICS INFO CTR BATTELLE COLUMBUS DIVISION 505 KING AVENUE COLUMBUS, OH 43201-2693	1

NOTE: PLEASE NOTIFY COMMANDER, ARMAMENT RESEARCH, DEVELOPMENT, AND ENGINEERING CENTER, US ARMY AMCCOM, ATTN: BENET LABORATORIES, SMCAR-CCB-TL, WATERVLIET, NY 12189-4050, OF ANY ADDRESS CHANGES.